International Journal of Nanomedicine

Dovepress
open access to scientific and medical research

Open Access Full Text Article

ORIGINAL RESEARCH

Orally Administered Halofuginone-Loaded TPGS Polymeric Micelles Against Triple-Negative Breast Cancer: Enhanced Absorption and Efficacy with Reduced Toxicity and Metastasis

Runan Zuo[1], Yan Zhang[1], Xiaorong Chen[1], Shiheng Hu[1], Xinhao Song[1], Xiuge Gao[1], Jiahao Gong[1], Hui Ji[1], Fengzhu Yang[1], Lin Peng[1], Kun Fang[2], Yingjun Lv[1], Junren Zhang[1], Shanxiang Jiang[1], Dawei Guo[1]

[1]Engineering Center of Innovative Veterinary Drugs, Center for Veterinary Drug Research and Evaluation, MOE Joint International Research Laboratory of Animal Health and Food Safety, College of Veterinary Medicine, Nanjing Agricultural University, Nanjing, 210095, People's Republic of China; [2]The First Affiliated Hospital of USTC, Division of Life Sciences and Medicine, University of Science and Technology of China, Hefei, 230001, People's Republic of China

Correspondence: Dawei Guo; Shanxiang Jiang, Engineering Center of Innovative Veterinary Drugs, Center for Veterinary Drug Research and Evaluation, MOE Joint International Research Laboratory of Animal, Health and Food Safety, College of Veterinary Medicine, Nanjing Agricultural University, 1 Weigang, Nanjing, 210095, People's Republic of China, Tel +86 25-84396215, Fax +86-25-84398669, Email gdawei0123@njau.edu.cn; nauvy@sina.com

Background: Halofuginone (HF)-loaded TPGS polymeric micelles (HTPM) were successfully fabricated using the thin-film hydration technique. HTPM via intravenous injection have been demonstrated to exert an excellent anticancer effect against triple-negative breast cancer (TNBC) cells and subcutaneous xenografts. In the present study, we further explored the potential treatment effect and mechanism of orally administered HTPM alone and in combination with surgical therapy on TNBC in subcutaneous and orthotopic mouse models.

Methods: Herein, the stability and in vitro release behavior of HTPM were first evaluated in the simulated gastrointestinal fluids. Caco-2 cell monolayers were then used to investigate the absorption and transport patterns of HF with/without encapsulation in TPGS polymeric micelles. Subsequently, the therapeutic effect of orally administered HTPM was checked on subcutaneous xenografts of TNBC in nude mice. Ultimately, orally administered HTPM, combined with surgical therapy, were utilized to treat orthotopic TNBC in nude mice.

Results: Our data confirmed that HTPM exhibited good stability and sustained release in the simulated gastrointestinal fluids. HF was authenticated to be a substrate of P-glycoprotein (P-gp), and its permeability across Caco-2 cell monolayers was markedly enhanced via heightening intracellular absorption and inhibiting P-gp efflux due to encapsulation in TPGS polymeric micelles. Compared with HF alone, HTPM showed stronger tumor-suppressing effects in subcutaneous xenografts of MDA-MB-231 cells when orally administered. Moreover, compared with HTPM or surgical therapy alone, peroral HTPM combined with partial surgical excision synergistically retarded the growth of orthotopic TNBC. Fundamentally, HTPM orally administered at the therapeutic dose did not cause any pathological injury, while HF alone led to weight loss and jejunal bleeding in the investigated mice.

Conclusion: Taken together, HTPM could be applied as a potential anticancer agent for TNBC by oral administration.

Keywords: triple-negative breast cancer, Halofuginone hydrobromide, TPGS polymeric micelles, subcutaneous xenografts, orthotopic xenografts, oral administration

Introduction

Triple-negative breast cancer (TNBC) is a particularly aggressive subtype of breast cancer that accounts for 10–20% of all invasive breast cancers.[1] TNBC is characterized by its more invasive nature, greater recurrence and metastasis potentials, and poorer outcomes compared with other major subtypes of breast cancer.[2,3] TNBC is not sensitive to endocrine therapy or HER-2–targeted treatment due to the absence or minimal expression of estrogen receptor (ER), progesterone receptor (PR), and human epidermal growth factor receptor 2 (HER-2) in TNBC cells.[4,5] Current treatment

Received: 4 December 2021
Accepted: 27 April 2022
Published: 30 May 2022

Graphical Abstract

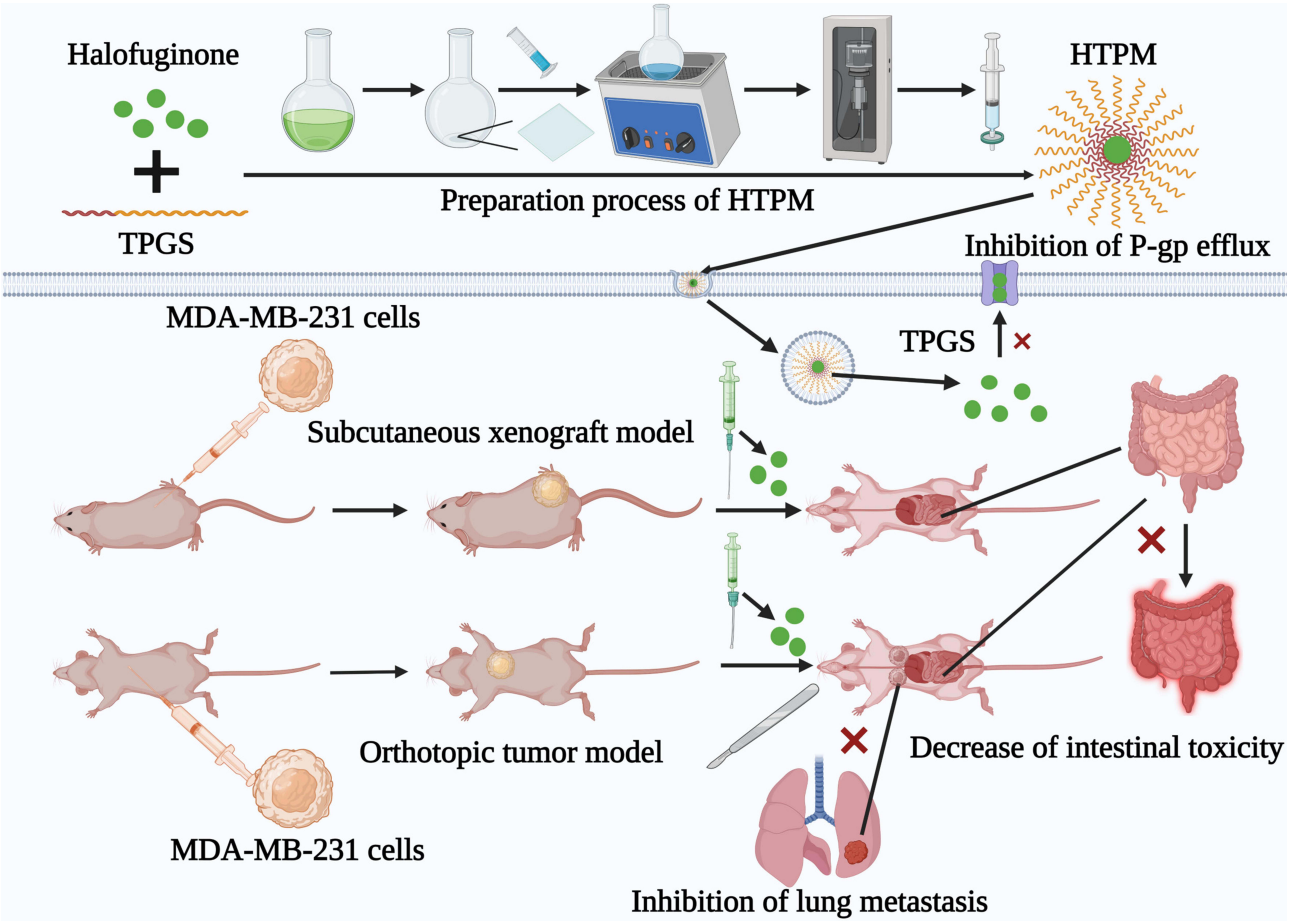

options for patients with TNBC include a combination of surgery, radiotherapy, and/or systemic chemotherapy. While chemotherapy remains the standard treatment for TNBC,[6] resistance to chemotherapy frequently develops, which results in a high mortality rate. Therefore, there is an urgent clinical need to develop novel therapeutic strategies for TNBC to improve survival rates in this patient population.

Halofuginone hydrobromide (HF) is a synthetic analogue of febrifugine derived from the Chinese herb *Dichroa febrifuga*.[7] It has been used to prevent coccidiosis in poultry and treat human scleroderma, as approved by the US Food and Drug Administration (FDA). In the past two decades, HF attracted increasing attention owing to its beneficial biological effects, including antifibrotic,[8] anti-inflammatory and autoimmune activities,[9] as well as antiproliferative, antiangiogenic, and anti-metastatic effects against multiple types of cancers, as demonstrated in several preclinical studies.[10,11] Moreover, HF has been tested for use as an anticarcinogenic agent for advanced solid tumors in a Phase I clinical trial.[12] It is well known that numerous nanocarriers, including polymeric micelles, could be utilized as excellent drug delivery systems of anticancer agents for enhancing solubility and permeability, augmenting bioavailability, reducing side effects, and increasing therapeutic efficiency.[13–16] Recently, we have demonstrated that encapsulating HF in TPGS polymeric micelles (HTPM) enhance the efficacy against subcutaneous TNBC xenografts of nude mice after intravenous administration.[17] However, oral administration is a considerably more convenient route and is often more acceptable to patients, especially for those who need to receive medications repeatedly, but is not always as efficient as other, more invasive routes. Generally, the kinetics of drug absorption and distribution may vary significantly between the different routes of administration, and bioavailability following oral

administration may be relatively lower.[18] In mice, HF is not detected in plasma and red blood cells after oral administration; however, it is easily detectable in the kidneys, liver, and lungs, and persists in these tissues for up to 48 hours, suggesting its limited oral bioavailability as well as its rapid and wide distribution.[19] As shown in a phase I clinical study in patients with advanced solid tumors, therapeutically effective plasma levels of orally administered HF can be achieved at a dosage that is well tolerated.[12] The "acute" maximum tolerated dose (MTD) is reached at 3.5 mg/day, and the dose-limiting toxicities (DLT) include nausea, vomiting, and fatigue. At present, HF in a sustained-release formulation to avoid any DLT is being evaluated in an FDA-approved phase 1b open-label, single- and multiple-ascending–dose study.[20] Consequently, the therapeutic potential of HTPM administered by oral gavage against TNBC should be further investigated in subcutaneous tumor mouse models.

Surgery is one of the important local treatments for breast cancer patients. Surgical treatment can remove tumor lesions and achieve radical treatment of breast cancer to a certain extent. In terms of local treatment, both breast-conserving surgery and total mastectomy have an increased risk of local recurrence or distant metastasis, and make no difference in overall survival.[21] Thus, based on the highly malignant characteristics of TNBC, local treatment combined with chemotherapy is beneficial for abating the risk of tumor recurrence.[22] Tumor metastasis requires a local niche to maintain tumor growth, while a metastatic niche contains various extracellular matrix (ECM) components and enzymes that contribute to the colonization and proliferation of disseminated cancer cells at a distant site.[23] Significantly, growing data have shown that HF can block the transforming growth factor beta (TGF-β) signaling pathway by inhibiting the phosphorylation and activation of Smad2 and Smad3, and also by inducing Smad7 expression.[24] It is well known that the production of ECM and epithelial–mesenchymal transition (EMT) of cancer cells can be activated by the TGF-β signaling pathway,[25] and thus, inhibition of TGF-β signaling by HF could effectively impede cancer invasion and metastasis.[26] Therefore, it is necessary to explore the efficacy of surgical treatment combined with HF chemotherapy on TNBC orthotopic tumors.

In the current study, the stability and in vitro release behavior of HTPM were first evaluated in the simulated gastrointestinal (GI) fluids. Caco-2 cell monolayers were then used to investigate the absorption and transport patterns of HF with/without encapsulation in TPGS polymer micelles. Subsequently, the therapeutic effect of orally administered HTPM was examined in subcutaneous tumor xenografts of TNBC in nude mice. Ultimately, orally administered HTPM combined with surgical therapy were utilized to treat TNBC in mouse orthotopic tumors. This study aimed to confirm the potential of HTPM as a novel oral therapeutic formulation against TNBC.

Materials and Methods

Materials and Reagents

Halofuginone hydrobromide (HF) was provided by Shanxi Meixilin Pharmaceutical Co., Ltd. (Yuncheng, China). D-α-tocopherol polyethylene glycol 1000 succinate (TPGS) was purchased from Guangzhou Kafen Biological Technology Co., Ltd. (Guangzhou, China). Fetal bovine serum (FBS) was provided by Gibco Laboratories (Grand, Island). Dulbecco's modified Eagle's medium (DMEM), trypsin, penicillin, and streptomycin were obtained from Hyclone Laboratories (Logan, UT). Bcl-2, Bax, and Caspase-3 antibodies were bought from Abcam Biotechnology Co., Ltd. (London, England). TUNEL kit was purchased from Nanjing Kai-ji Biotech Co., Ltd. (Nanjing, China), while the immunohistochemistry kit was bought from Abcam Biotechnology Co., Ltd. (London, England). All other reagents and chemicals were of analytical grade without further purification.

Cell Line Culture

Colorectal carcinoma cell line Caco-2 and breast cancer cell line MDA-MB-231 were maintained in DMEM supplemented with 1% penicillin, 1% streptomycin, and 10% FBS in a cell incubator with 5% CO_2 at 37°C. These cells were purchased from the Type Culture Collection of the Chinese Academy of Sciences (Shanghai, China).

Preparation and Characterization of HF-Loaded TPGS Polymeric Micelles

It has been reported that TPGS could self-assemble to form nano-micelles with critical micellar concentration (CMC) of 13.91 μg/mL.[27] Herein, HTPM were prepared using the thin-film hydration method as reported previously.[17] Briefly, HF and TPGS were first dissolved in methanol to obtain the transparent organic phase. Then, the organic phase was gradually

evaporated to form a thin film on the surface of the distillation flask. The deionized water was further added into the distillation flask; then, an ultrasonic cell disruption device (JY96-II, Xin zhi Biotechnology Co., Ltd., Ningbo, China) (300 mV, 20 min) was used to acquire HTPM. The hydrodynamic diameter (HD), *zeta* potential (ZP), and polydispersity index (PDI) of the HTPM were measured by dynamic light scattering (DLS) with a Zeta-sizer (Nano ZS90; Malvern Instruments Ltd., Malvern, New York, USA). The samples at appropriate concentrations were determined with scattering angles of 90° at 25°C. The morphology was observed by transmission electron microscopy (TEM, JEM-1200EX; JEOL, Tokyo, Japan).

The stability of HTPM were evaluated in the simulated gastric fluids with pepsin (pH 1.2) and simulated intestinal fluids with trypsin (pH 6.8). Briefly, HTPM were first incubated with the simulated GI fluids at 37°C. The HD and ZP of HTPM were then analyzed every hour for the first two hours and for 24 hours.

The in vitro release profiles of HTPM were examined in the simulated GI fluids. The HTPM (5 mL) were sealed in dialysis bags, and then immersed in the simulated gastric or intestinal fluids (500 mL) at 37°C under magnetic stirring with 100 rpm. The release medium (1 mL) was taken out at predetermined time intervals and replaced with the same amount of fresh release medium. The concentrations of HF in the release medium were determined using UV spectrophotometry (UV-1900; Shimadzu Instruments, Suzhou, China).

Transport Studies of HTPM Across Caco-2 Cell Monolayers

Caco-2 cells were cultured in DMEM supplied with 10% (v/v) FBS and 1% (v/v) penicillin–streptomycin mixture at 37°C under a 5% CO_2 atmosphere. For transport experiments, the cells were seeded at a density of 2×10^5 cells per well on Transwell® polycarbonate inserts (12-well and 0.4-μm pore diameter; Corning Costar, Cambridge, MA, USA) to establish the cell monolayers, the integrity of which was ensured by measuring the transepithelial electrical resistance (TEER) with an epithelial volt ohmmeter (Millipore, Burlington, MA, USA). The cell monolayers were utilized for transport studies only when TEER values were over 500/cm^2. The transport experiments were performed by adding the HF or HTPM solution (2 μg/mL) to either the apical (AP, 0.5 mL) or basolateral side (BL, 1.5 mL), while the receiving compartment contained the corresponding volume of the transport medium. After incubation at 37°C for four hours, the transfer fluids were collected from the BL or AP side and taken to detect HF concentrations by high-performance liquid chromatography (HPLC). To demonstrate whether HF is a substrate of drug efflux transporter P-glycoprotein (P-gp) and examine the effect of HTPM on the absorption of HF, the cell monolayers were preincubated with a P-gp inhibitor verapamil (100 μM) for one hour, and HF or HTPM were then added into the AP or BL sides, respectively; the verapamil was then co-incubated with HF or HTPM for four hours for the bidirectional transport assay. The apparent permeability coefficient (P_{app}) and efflux ratio (ER) of bidirectional transport of HF and HTPM were subsequently compared and analyzed to evaluate the permeability of HTPM. The P_{app} and ER were calculated according to the following equations:[28,29]

$$P_{app} = dQ/dt \times AC_0$$

where dQ/dt is the amount of drug transported per unit time, A is the membrane area of the transwell® cell, and C_0 is the concentration of the drug before transport;

$$ER = P_{app}(BL \rightarrow AP)/P_{app}(AP \rightarrow BL)$$

where P_{app}(BL→AP) is the permeability coefficient on the BL→AP side, while P_{app}(AP→BL) is the permeability coefficient on the AP→BL side.

To investigate the internalization mechanism of HTPM, the cell monolayers were pretreated with diverse endocytosis inhibitors, including chlorpromazine (CPZ) (30 μM), MβCD (2 mM), and EIPA (50 μM).[30,31] After one hour, HTPM (0.5 mL) were supplemented on the AP side and co-incubation was continued with the cells for four hours. HTPM without any inhibitors were utilized as the control group. Finally, the obtained transfer fluids from the BL side were used for HPLC analysis. In addition, one-way transport on the AP→BL side at 4°C was set up to investigate the role of energy during transport.

Animal Experiments

BALB/c nude mice (four weeks old, female) were purchased from the Comparative Medicine Laboratory Animal Center of Yangzhou University (Yangzhou, China), and reared in the Laboratory Animal Center of Nanjing Agricultural University (NJAU). All of the animal experiments were performed in accordance with the Guidelines for Animal Experimentation of NJAU, and the research protocols of subcutaneous and orthotopic TNBC xenograft models were approved by the Animal Ethics Committee of NJAU (No. 20191217004, 20210317022).

Therapeutic Effect of HTPM Administered Orally on Subcutaneous TNBC in Nude Mice

A TNBC-bearing mouse model was successfully established by subcutaneous injection of MDA-MB-231 cells (1×10^6 cells/mouse) into the right thigh of BALB/c nude mice. When the tumor volumes reached 50–100 mm^3, the tumor-bearing mice were weighed and randomly assigned into three groups: control (PBS), HF, and HTPM. In the HF and HTPM groups, the mice were orally administered with the same dose of 0.25 mg/kg HF on days 0–14 (every two days). The tumor size and body weight for all of the mice were monitored every two days until the day 17. After the experiment, the animals were dissected to collect the main organs and tumor tissues for pathological analysis or TUNEL staining. The tumor inhibition rate (TIR) was calculated according to the following formula:

$$TIR = (1 - V_D/V_B) \times 100\%$$

where V_D and V_B represent the mean tumor size in the dosed group and control group, respectively.

Treatment Effect of Orally Administered HTPM Combined with Surgery on Orthotopic TNBC Mice

MDA-MB-231 cells (1×10^6 cells/mouse) were injected into the second pair of mammary glands on the right to establish the orthotopic TNBC mouse models.[32,33] The width and length of the tumors were measured using vernier caliper, and the tumor volume was calculated using the formula $V = (a \times b^2)/2$, where a and b represent the longest length and the relatively shorter width of the tumor, respectively. When the tumor size reached 80–100 mm^3, we performed surgical resection of the tumors on a sterile operating table. Briefly, the mice were exposed to inhalation anesthesia with isoflurane and placed in a supine position, and the skin of the axillary breast was disinfected with 75% alcohol. A small incision with about 1 cm in length in the breast was made to remove a part of the tumor, 5–10% of which was left in the body (black arrows were used to mark residual tumors in the mice) (Supplementary Materials, Figure S1). The incision was sutured with 5-0 sutures, and the wound was treated with iodophor. The mice were kept warm and closely monitored until they awoke.

Twenty mice undergoing surgical resection were randomly divided into four groups as follows: tumor resection surgery (TRS)+PBS, TRS+TPGS polymeric micelles without HF (FTPM), TRS+HF, and TRS+HTPM. Then, the nude mice were orally administered with the same volume of either PBS, FTPM, HF, or HTPM on days 0–14 (every two days). The tumor size and body weight for each mouse were measured every two days until day 17. At the end of the experiment, the animals were dissected to collect the main organs and tumor tissues for pathological analysis or TUNEL staining.

TUNEL Staining of Tumor Tissues

TUNEL staining was utilized to detect apoptosis in the tumor tissues. Briefly, paraffin-embedded sections were deparaffinized, and proteinase K (20 μg/mL, 100 μL) was added to each slide to cover the tissue sections. The slides were incubated at room temperature for 10 to 30 minutes, rinsed three times with PBS, and then blocked by peroxidase for 30 minutes. TdT (50 μL) and dUTP (450 μL) were mixed uniformly to prepare TUNEL reaction solution, 50 μL of which was subsequently placed onto the specimen and reacted for one hour in a dark humidified chamber at 37°C. After washing three times with PBS, labeled horseradish peroxidase (50 μL) was added dropwise to react for 30 minutes at 37°C without protecting from light, which was followed by washing three times with PBS. Next, diaminobenzidine (DAB) substrate was placed dropwise to initiate a coloration reaction at room temperature for 10 minutes, followed by washing three times with PBS. Next, hematoxylin counterstaining and hydrochloric acid alcohol differentiation were

conducted, and then lithium carbonate appeared blue for one minute due to hematoxylin counterstaining. Finally, the slides were rinsed in ethanol gradient solutions for dehydration, and xylene was utilized for ensuring transparency. The slides were sealed and examined under a fluorescence microscope. Cells with a nucleus stained with hematoxylin were blue, whereas the apoptotic cells developed by DAB reagent had a brown-yellow nucleus.

Immunohistochemistry of Animal Tissues

Immunohistochemistry was utilized to investigate the cell surface antigens of the tumor tissues. The paraffin-embedded sections mentioned above were dewaxed and rehydrated, and the tissue sections were then placed in a repair box filled with citric acid buffer (pH 6.0) for antigen retrieval in a microwave oven. Then, the sections were placed in 3% hydrogen peroxide and incubated at room temperature in darkness for 25 minutes. The sections were placed in PBS (pH 7.4) and shaken with a decolorizing shaker three times for five minutes. Moreover, 3% BSA was added to the center of the sections to evenly cover the tissues for 30 minutes at room temperature. Next, the sealing solution was gently removed; primary antibodies, such as Bcl-2, Bax, and Caspase-3 antibody, were incubated overnight at 4°C; and the sections were subsequently placed in PBS (pH 7.4) and washed by shaking on the decolorizing shaker three times for five minutes. After the sections were slightly shaken and dried, the tissues were covered with goat anti–rabbit antibody for incubation. Afterward, DAB chromogenic reaction and nuclear counterstaining were conducted. Eventually, the slices were dehydrated and sealed for visualization and analysis under the microscope. Nuclei stained with hematoxylin were blue, and those expressing the investigated antigens were brownish to yellow.

Statistical Analysis

GraphPad Prism 6.0 (La Jolla, CA, USA) was used to analyze the data. Student's *t*-test was utilized to evaluate the differences between the two groups. The data are shown as the mean ± standard deviation (M±SD). $*P < 0.05$, $**P < 0.01$, and $***P < 0.001$ were considered statistically significant, statistically extremely significant, and statistically the most significant, respectively.

Results and Discussion

Characterization of HTPM

Peroral drug delivery is the most convenient and preferred administration route for patients, especially when long-term or daily use is required. However, the poor water solubility of HF limits its oral delivery as an anticancer agent. Therefore, it is essential to design appropriate drug delivery systems for HF to achieve improved bioavailability and antitumor efficacy. At present, numerous nanoparticles, including liposome, nano-emulsion, nanosuspension, and many other nanocarriers, are available for oral delivery of antitumor drugs.[34] Among them, polymeric micelles (PMs) formed by self-assembly are one of the most promising delivery systems, and they have been developed to effectively deliver anticancer drugs by oral route.[35–37] Compared with other nanoparticles or nano-capsules, PMs have a higher drug loading capacity, stable structure, long retention time in the body, and few adverse effects.[38,39] Therefore, after being designed appropriately, PMs could be a promising drug carrier for oral delivery of HF.

TPGS not only shows outstanding drug delivery ability because of the special amphiphilic structure, but it can also be functionalized as an excellent solubilizer, bioavailability enhancer, and stabilizer of hydrophobic drugs due to its large surface area and bulky structure.[27] Herein, HTPM have been successfully prepared by the thin-film hydration method (Figure 1), as reported previously.[17] For oral delivery, the particle size and surface charge of the self-assembled micelles appear to be the most important parameters, which greatly influence the transport route of micelles through the intestinal epithelium membrane and determine their stability.[40] Thus, the HD, PDI, and ZP were determined by DLS. The optimal formulation of HTPM had an HD of 17.8 ± 0.5 nm (Figure 2A), which contributes to the penetration of and/or interaction with dense microvilli (microvillus diameter ~100 nm).[17] In addition, the PDI of HTPM was 0.212 ± 0.1, suggesting its high homogeneity. A recent investigation has shown that the ZP of drug-free TPGS polymer micelles was negative.[27] Herein, HTPM were positively charged, with a ZP of 14.40 ± 0.1 mV (Figure 2B), which may be due to the H^+ accumulated by amino in the molecule structure of HF. The positively charged HTPM could interact with the negatively

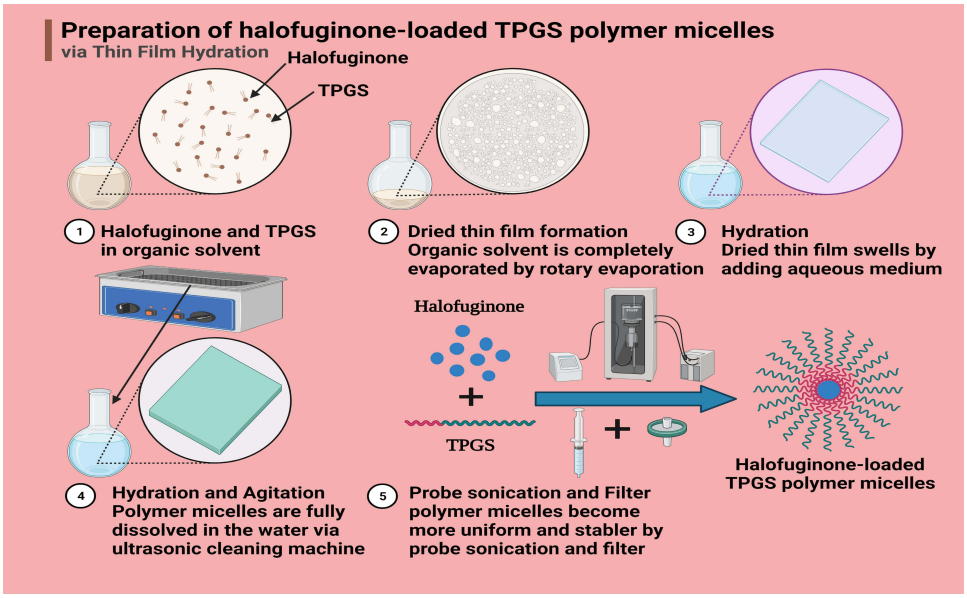

Figure 1 Preparation process of HTPM. HTPM were prepared using the thin-film hydration method as reported previously. Briefly, HF and TPGS were first dissolved in methanol to obtain the transparent organic phase. Then, the organic phase was gradually evaporated to form a thin film on the surface of the distillation flask. The deionized water was further added into the distillation flask; then, an ultrasonic cell disruption device (300 mV, 20 min) was used to acquire HTPM.

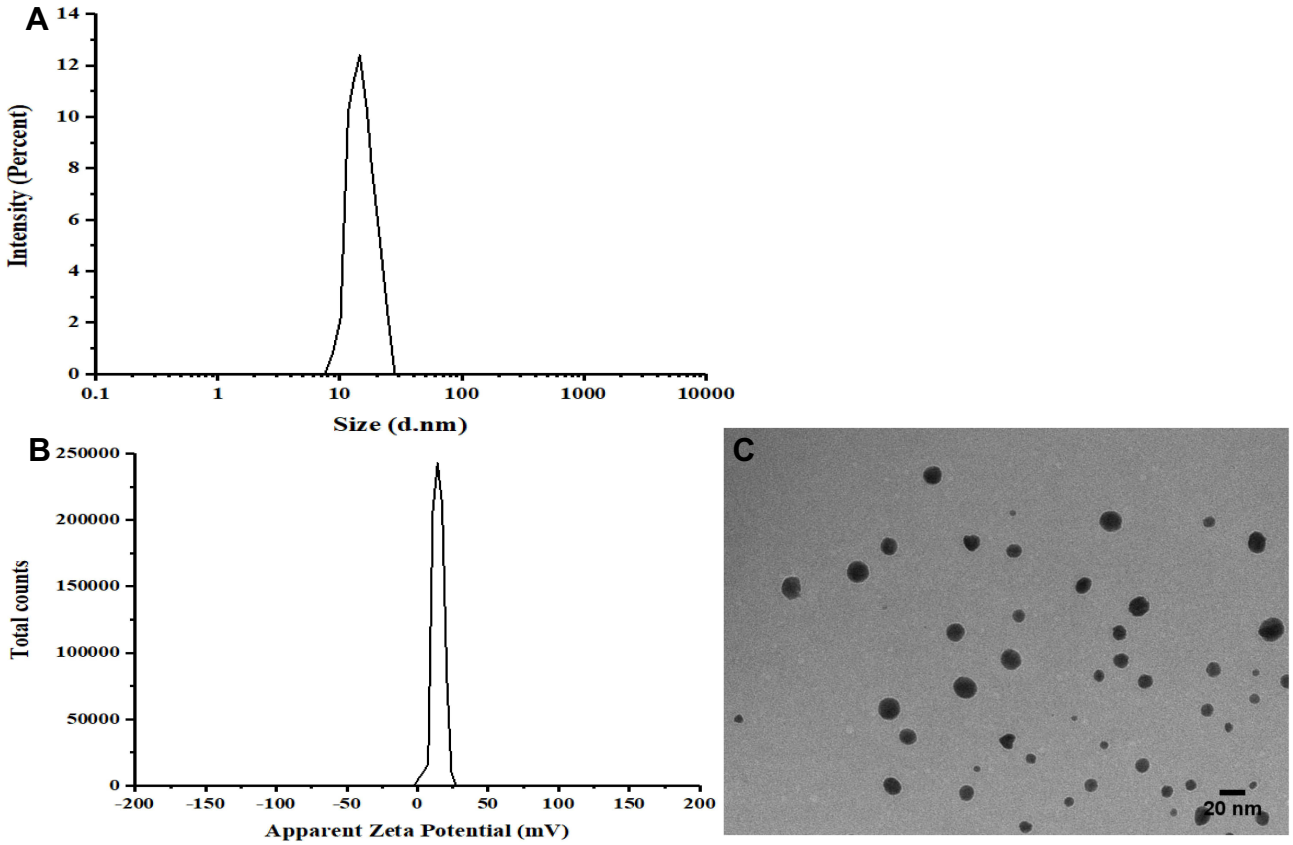

Figure 2 Characterization of HTPM. Hydrodynamic diameters (**A**) and *zeta* potentials (**B**) of HTPM were determined by dynamic light scattering. The surface morphology (**C**) of HTPM was observed by transmission electron microscopy (TEM).

charged intestinal mucus due to electrostatic interactions, thereby contributing to the prolonged intestinal retention time. Transmission electron microscopy (TEM) was applied to further observe the morphology of HTPM. HTPM appeared approximately spherical with uniform distribution (Figure 2C), implying their good stability.[41,42]

Stability of HTPM in GI Fluids

Our previous study demonstrated that compared with free HF, HTPM exhibited excellent storage stability, dilution tolerance, and sustained release in a pH-dependent manner.[17] Intended to be an oral delivery carrier, the stability of HTPM should be further investigated in the harsh GI environment to evaluate whether they are degraded before reaching the absorption sites. As shown in Figure 3B, the ZP of HTPM slightly varied with the pH change of the simulated GI fluids, and still remained positively charged in the simulated gastric fluids with pepsin (pH 1.2) and intestinal fluids with trypsin (pH 6.8). Furthermore, the HD of HTPM did not significantly change with the exposure to the simulated gastric fluids or intestinal fluids over 24 hours (Figure 3A). In addition, the weak interactions and steric repulsion interactions (electrostatic) among the TPGS molecules from nano-micelles improved the structural integrity of the self-assembly nanomicelles.[27] These data suggest that HTPM can maintain high stability in the simulated GI fluids.

In vitro Release of HTPM

As shown in our previous study,[17] HTPM possessed an encapsulation efficiency of 90.6% ± 0.85% and sustained release behaviors in PBS with varied pH values. Herein, the release profiles of HTPM in the simulated gastric fluids or

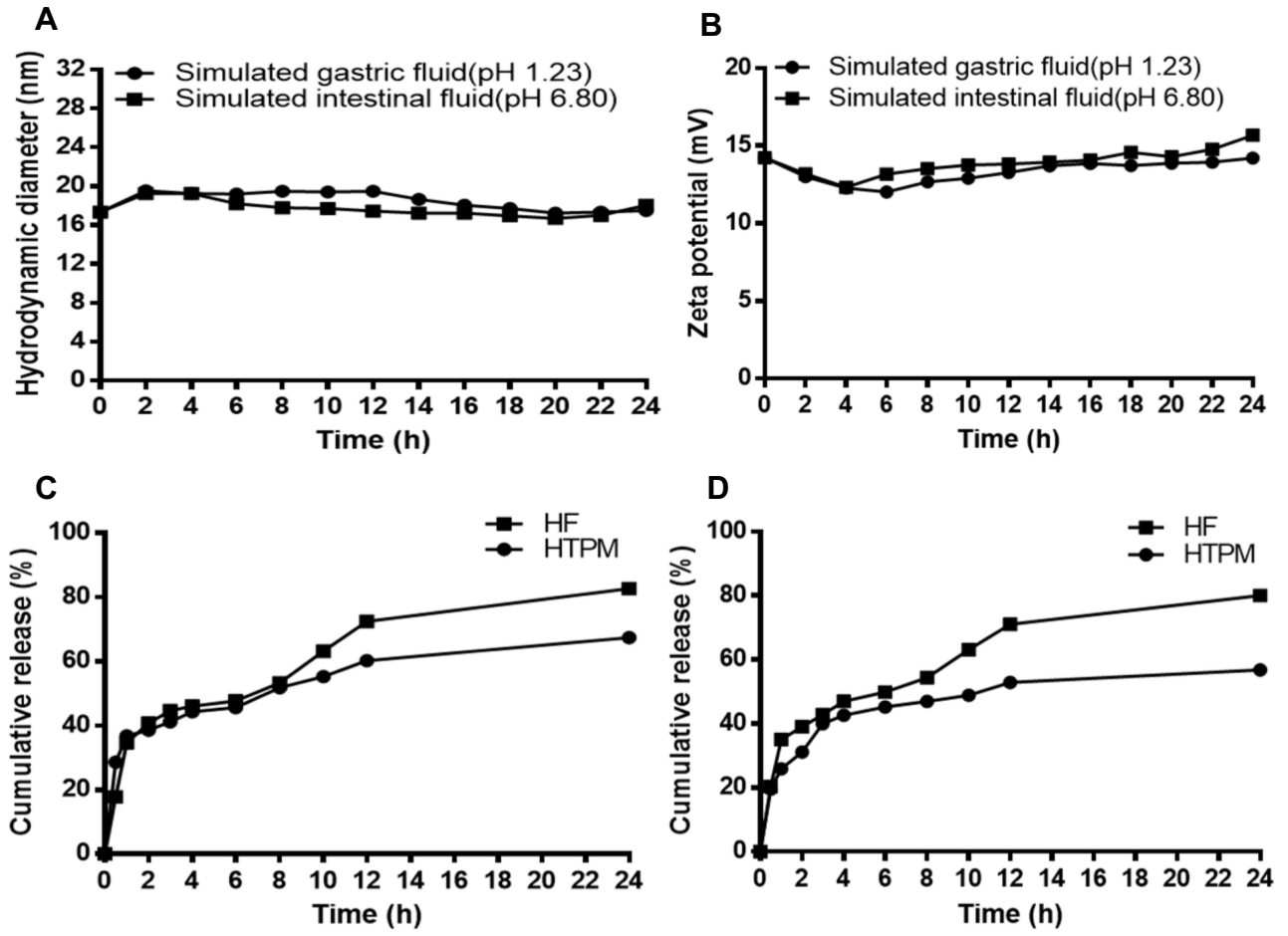

Figure 3 Stability of HTPM and in vitro drug release profiles of HF and HTPM in the simulated gastrointestinal fluids. The stability of HTPM in the simulated gastric (pH 1.23) and intestinal (pH 6.8) fluids were evaluated by the change of hydrodynamic diameter (**A**) and *zeta* potential (**B**) during 1-day storage. In vitro drug release profiles of HTPM and HF in the simulated gastric (**C**) and intestinal (**D**) fluids were investigated using the dialysis bag method.

intestinal fluids were further monitored using the dialysis bag technique to evaluate its potential of oral delivery. The results showed that the cumulative release percentage (CRP) of HF from HTPM was 56.72% within 24 hours in the simulated gastric fluids, while that of free HF was 80.03% (Figure 3C), indicating that HTPM had low release characteristics in a strong acidic environment. The CRP of HF from HTPM from 0 to 8 hours was 51.8%, while that of free HF was 53.25%, indicating the lack of obvious difference. However, the CRP of HF from HTPM from 8 to 12 hours was only 8.34%, while that of free HF was 19.6%, which revealed the sustained release. Furthermore, the CRP of HF from HTPM within 24 hours in the simulated intestinal fluids was 67.34%, while that of free HF was 82.61% (Figure 3D), suggesting the excellent sustained release kinetics of HTPM. The CRP of HF from HTPM from 0 to 8 hours was only 46.96%, while that of free HF was 54.39%, which demonstrated the slow release of HF from HTPM in the simulated intestinal fluids. Moreover, the CRP of HF from HTPM from 8 to 12 hours was only 5.88%, while that of free HF was 18.17%. Interestingly, HTPM exhibited a lower CRP in the simulated intestinal fluids than in PBS with similar pH, which may be due to protein corona formation by the adsorption of trypsin on the micelles' surfaces.[43]

Permeability and Transport Mechanism of HF Across Caco-2 Cell Monolayers

As depicted in Table 1, the efflux rate (ER) of HF in Caco-2 cell monolayers was 1.84, which was more than the value of 1.5 in FDA regulations;[44] this finding suggests that HF may be a substrate of P-gp. The P_{app} value (AP→BL) of HF markedly increased from $(4.73 \pm 0.28) \times 10^{-6}$ cm/s to $(6.25 \pm 0.75) \times 10^{-6}$ cm/s, while the P_{app} value (BL→AP) decreased from $(8.72 \pm 0.16) \times 10^{-6}$ cm/s to $(5.9 \pm 0.1) \times 10^{-6}$ cm/s, and the corresponding ER value decreased to 0.94 upon incubation with a typical P-gp inhibitor verapamil, thereby further corroborating HF as the substrate of P-gp.[45] The efflux transporters expressed in the intestinal cells can limit drug absorption.[46] It is well known that TPGS can suppress the efflux of P-gp by inhibiting the ATPase activity.[47] In the present study, we found that the P_{app} value (AP→BL) of HTPM was significantly increased, while their P_{app} value (BL→AP) was markedly decreased compared with that of HF (Figure 4A and B), and the resultant ER of HTPM was reduced to 1.21, demonstrating that polymeric micelles self-assembled by TPGS can inhibit the efflux of P-gp against HF in Caco-2 cell monolayers. Incubation with verapamil further influenced the bidirectional P_{app} value and ER of HTPM, but there was no significant change compared with that of HTPM alone. Generally, HTPM can increase the absorption of HF by Caco-2 cells (AP→BL) and reduce the efflux of P-gp on HF (BL→AP) to improve the permeability to HF in Caco-2 cells.

As displayed in Figure 4C, the P_{app} values of HF and HTPM at 4°C were lower than those at 37°C. Low temperature is a known inhibitor of cell metabolism, and the uptake of a tracer via pinocytic/endocytic route is inactivated at 4°C.[48] Therefore, it was predicted that HTPM mainly entered Caco-2 cells via an energy-dependent active transport mode. The endocytic pathways of nanoscale systems include phagocytosis, clathrin-dependent endocytosis, caveolae-mediated endocytosis, clathrin/caveolae-independent endocytosis, and macropinocytosis.[28,49,50] Hence, various endocytic inhibitors were utilized to pretreat Caco-2 cells so as to investigate the mechanism of HTPM entrance into cells (Figure 4D). The results showed that the P_{app} value of HTPM co-incubated with MβCD was significantly reduced compared with that of HTPM without any inhibitors, while neither chlorpromazine nor EIPA produced significant changes in the P_{app} value

Table 1 Permeability and Efflux Rate (ER) of HF and HTPM Transport into Caco-2 Cell Monolayers

Reagents	Concentration (μg/mL)		P_{app} ($\times 10^{-6}$cm/s)		Efflux Rate (ER)
			AP→BL	BL→AP	
HF	–	2	4.73±0.28	8.72±0.16	1.84
	+		6.25±0.75*	5.9±0.1**	0.94
HTPM	–		5.72±0.31*	6.91±0.44**	1.21
	+		5.88±0.28**	6.56±0.48**	1.12

Notes: "+" and "-": treatment with/without verapamil; P_{app} values in the same column are compared with that in the first row. $P < 0.05$ means significant difference marked with*, and $P < 0.01$ represents extremely significant difference marked with**.

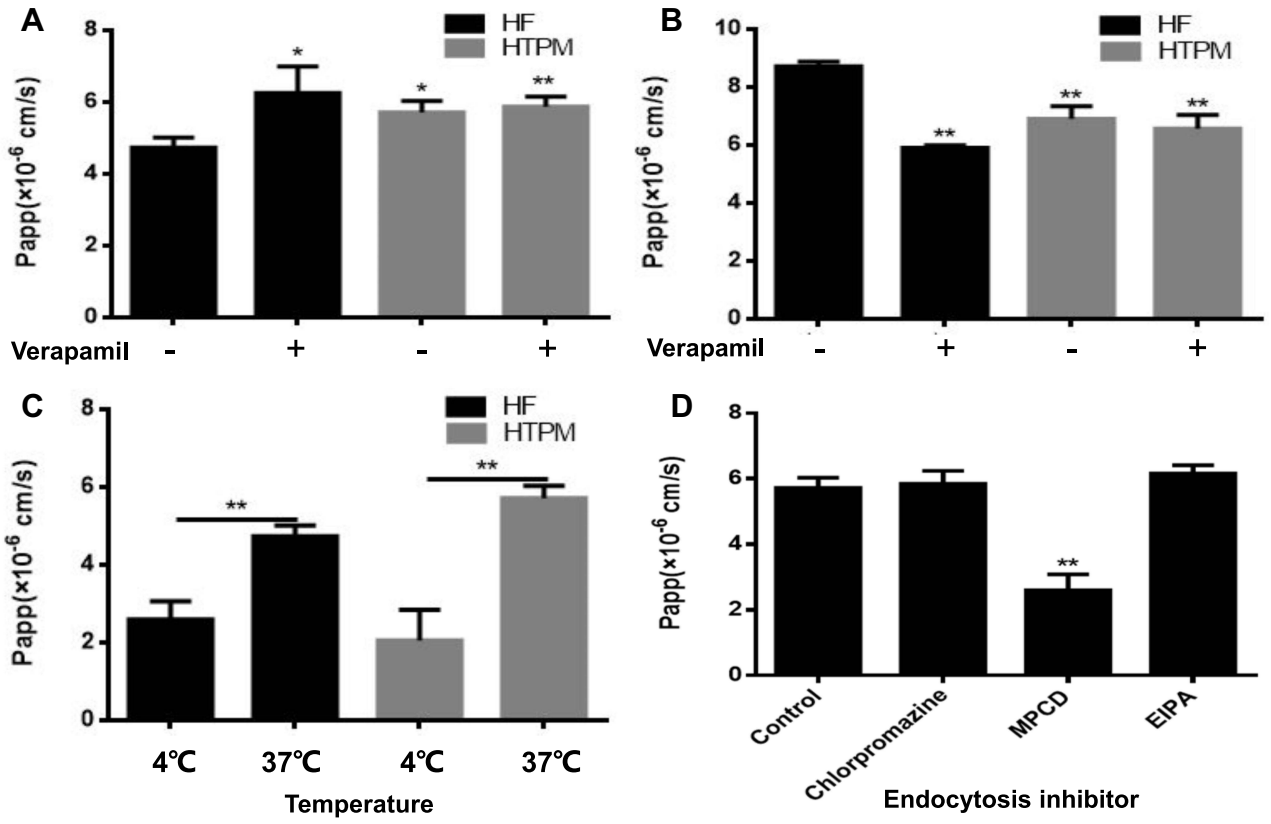

Figure 4 Permeability and transport patterns of HTPM across Caco-2 cell monolayers. The P_{app} values of HF and HTPM treated with (+) /without (-) verapamil were detected in the AP→BL side (**A**) and BL→AP side (**B**), respectively. Effect of temperature on the P_{app} of HTPM across Caco-2 cells monolayer was studied at 4°C and 37°C (**C**). Effect of various endocytosis inhibitors on the P_{app} values of HTPM (**D**) was analyzed. *P < 0.05, **P < 0.01.

of HTPM. These data indicate that HTPM enter Caco-2 cells mainly through a caveolin/lipid raft–mediated endocytic pathway.

Antitumor Effect in vivo

Therapeutic Effect of Orally Administered HTPM on Subcutaneous TNBC Xenografts

Effects of orally administered HF and HTPM on the growth of subcutaneous TNBC xenografts were investigated (Figure 5A). MDA-MB-231 cells (1×10^6 cells/mouse) were implanted subcutaneously in BALB/c nude mice, which were given HF or HTPM (0.25 mg/kg) by gavage when the tumor volume was 50–100 mm^3. The tumor size of all of the groups gradually enlarged as a function of time, and a significant reduction in tumor size was observed in the HF-treated nude mice 12 days after oral administration in comparison to the untreated mice. More interestingly, the TIR value of HTPM treatment was 70.19% ± 1.56%, whereas that of HF treatment was only 47.55% ± 1.32%, indicating that HTPM achieved stronger inhibition of the tumor progression than did HF (Figure 5B). The mice were euthanized and dissected to collect the tumor samples on day 17, and photographs were taken (Figure 5C). The tumor weights in the HTPM-treated group were much lower than those in the groups treated with PBS or HF (Figure 5D). These data indicated that HTPM exhibited stronger anticancer efficacy toward breast cancer than free HF. A previous pharmacokinetics study has suggested limited oral bioavailability of HF in CD2F1 mice and Fischer 344 rats.[19] PMs could enhance the oral bioavailability and antitumor efficacy of poorly soluble drugs.[51,52] Hence, TPGS polymeric micelles could improve the inhibitory effect of HF against breast cancer, although this needs to be confirmed in a follow-up pharmacokinetics study.

H&E staining of the tumor sections (Figure 6) revealed that tumor samples treated with HF or HTPM had a larger necrotic area than those from the PBS group, and tumors from the HTPM-treated group had the maximum amount of necrosis. Furthermore, TUNEL staining of the tumor tissues clearly detected higher apoptosis induced by HTPM

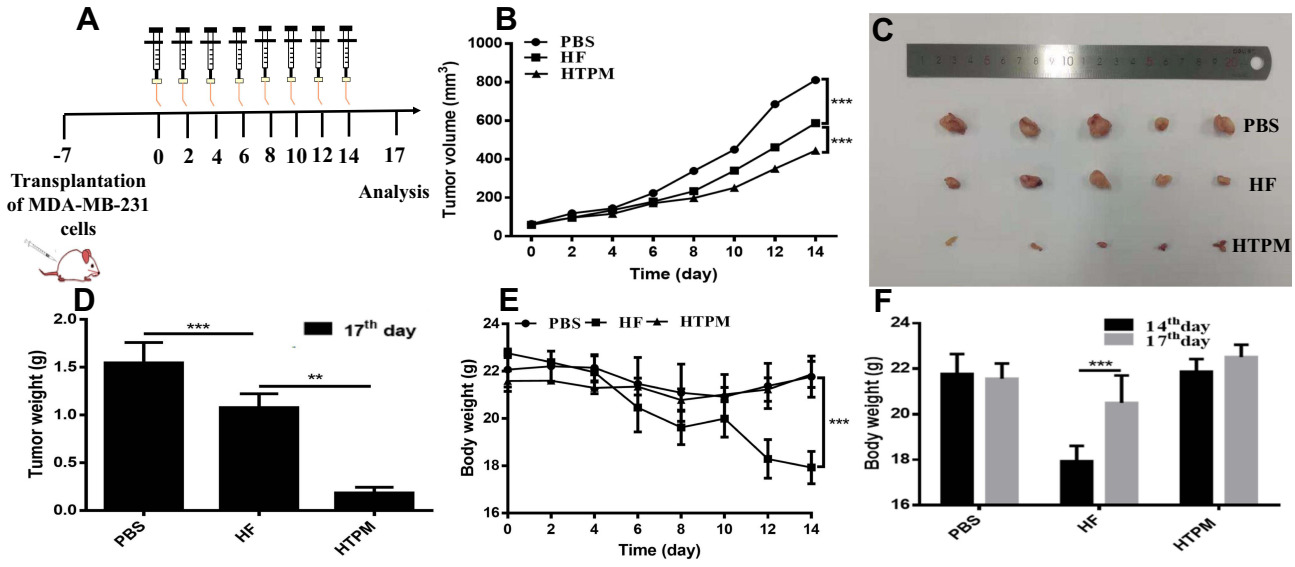

Figure 5 Anticancer effect of HTPM orally administrated against subcutaneous TNBC xenografts in nude mice. Pattern diagram (**A**), tumor volumes (**B**), morphology of the harvested tumors (**C**), tumors weights (**D**), body weights (**E** and **F**) of nude mice after oral administration of PBS, HF, or HTPM were exhibited. $^{**}P < 0.01$, $^{***}P < 0.001$.

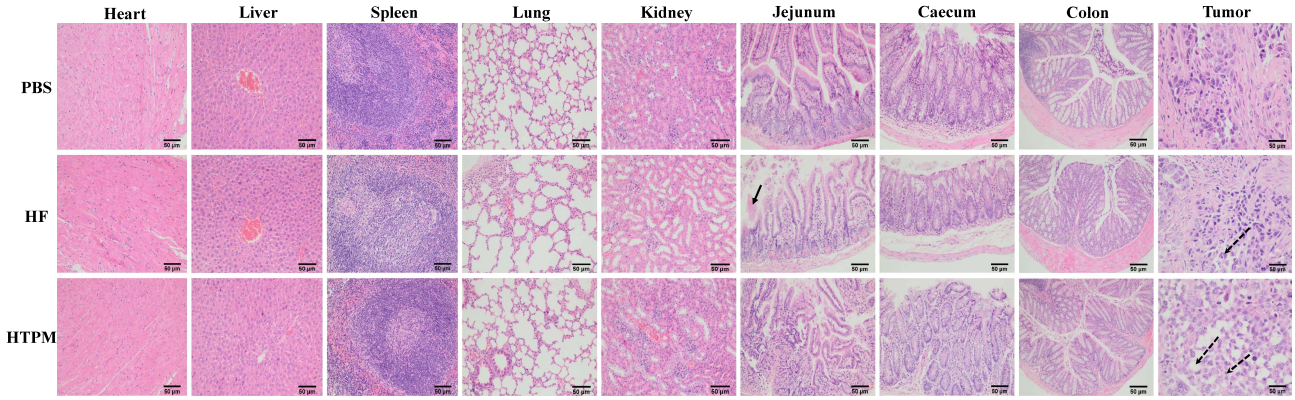

Figure 6 Histological analysis of main organs and tissues from subcutaneous tumor-bearing mice treated with HTPM orally administrated. All the samples were analyzed using H&E staining. The place pointed by the black solid arrow in the jejunum picture of HF group represents the phenomenon of jejunum hemorrhage. Further, places pointed by the black dotted arrow in the tumor picture of HF group and HTPM group demonstrate generation of apoptosis for tumor tissues. Images were taken at 200× magnification.

compared with other treatments. To determine the apoptotic potential of any compound, evaluation of Bax/Bcl-2 ratio is an important parameter, where a high Bax/Bcl-2 ratio indicates cells with apoptotic features. Additionally, Bax/Bcl-2 ratio is correlated with the increase in caspase-3 activity. Consequently, the levels of apoptosis-related proteins such as Bcl-2, Bax, and Caspase-3 were determined in the tumor issues by immunohistochemistry. As shown in Figure 7, HF markedly upregulated the expression of Bax and Caspase-3, and downregulated the expression of Bcl-2. More importantly, these changes were further augmented by HTPM. Collectively, these data indicated that HTPM could enhance the inhibitory effect of HF against the growth of TNBC xenografts.

The in vivo toxicity of these treatments was also monitored by the change in body weight and histologic analysis of major organs. Oral administration of HF caused the loss of body weight in mice, but this phenomenon was not found in PBS or HTPM (Figure 5E), or in the intravenous injection of HF in our previous study.[17] Furthermore, the body weight of nude mice rapidly increased three days after the withdrawal of HF (Figure 5F). According to the H&E staining, congestion was found only in the jejunum of some mice, and no lesions appeared in other major organs and tissues,

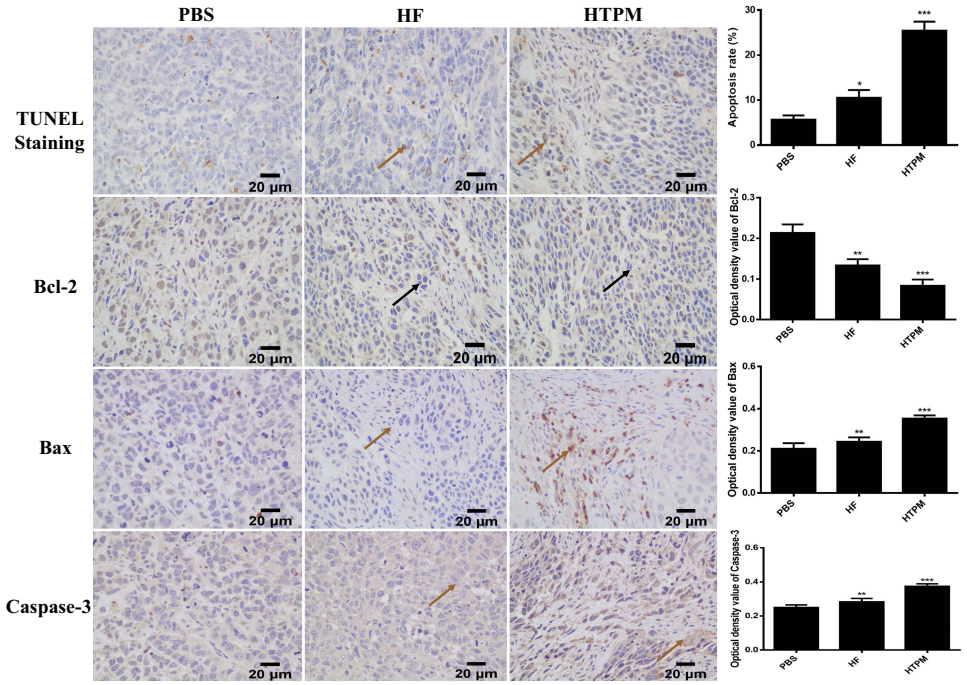

Figure 7 Apoptosis of tumor tissues from subcutaneous tumor-bearing mice treated with HTPM orally administrated. TUNEL staining was utilized to detect the apoptosis of tumor tissues, and the expression of apoptosis-related proteins including Bcl-2, Bax and Caspase-3 were investigated using immunohistochemistry. Places pointed by the brown solid arrow in the TUNEL Staining, bax and caspase-3 for HF and HTPM represent generation of apoptosis for tumor tissues, which appear brown color. Furthermore, Places pointed by the black solid arrow in the bcl-2 for HF and HTPM indicate anti-apoptosis for tumor tissues. Images were taken at 400× magnification. *$P < 0.05$, **$P < 0.01$, ***$P < 0.001$.

including the heart, liver, spleen, lung, kidney, cecum, and colon. It has been reported that HF predominantly causes GI toxicity consisting of nausea and vomiting in patients with advanced solid tumors, which is chronologically related to the oral administration of the drug.[12] Most patients experience nausea and vomiting within 30 minutes to one hour after ingestion of the drug. Several patients experienced bleeding complications during treatment with HF, including gastric, intestinal, and hepatic bleeding. The high number of observed bleeding events points to a possible relationship with the oral administration of HF, and thus chronic administration at the dose of 0.5 mg/day is recommended for Phase II clinical studies.[12] In the current study, HTPM did not lead to body weight loss and breeding of nude mice, which may be due to its high encapsulation efficiency and sustained release behavior in the intestines mentioned above.

Combined Therapeutic Effect of Orally Administered HTPM and Surgery on Orthotopic TNBC in Nude Mice

To evaluate the combined effect of orally administered HTPM and surgery on the TNBC growth within the breast microenvironment, MDA-MB-231 cells were injected into the second pair of mammary glands on the right to establish the orthotopic TNBC in nude mice.[53] As displayed in Figure 8A, resident tumor tissues continued to enlarge as a function of time after surgical resection. No complete growth arrest but rather a significant delay in tumor growth was observed in HF- and HTPM-treated mice compared with the PBS- and FTPM-treated groups, although the tumor tissues had become smaller due to surgical resection. Furthermore, we also found that the TIR value of HTPM treatment was 72.24% ± 1.56%, whereas that of HF treatment was only 43.57% ± 1.15%, suggesting the HTPM group significantly outperformed the HF group in tumor inhibition. The mice were euthanized and dissected to collect the tumor samples on day 17, and photographs were taken (Figure 8B). The tumor weights in the HTPM-treated group were the lowest among the treated groups (Figure 8C). Subsequently, the in vivo toxicity of these treatments, especially in the TRS+HF group, was also observed as the alteration in body weight. Namely, oral administration of HF caused the loss of body weight (Figure 8D)

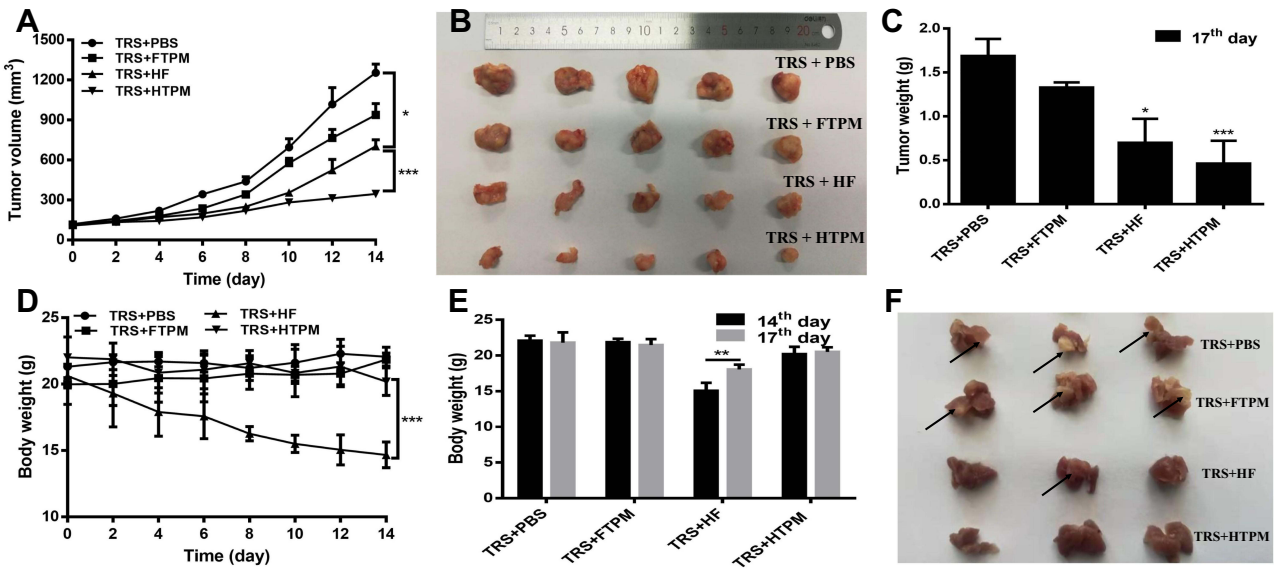

Figure 8 Therapeutic effect of HTPM administrated orally combined and surgery on orthotopic TNBC in nude mice. Tumor volumes (**A**), morphology of the harvested tumors (**B**), tumors weights (**C**), body weights (**D** ând **E**) and morphology of lung metastasis (**F**) of orthotopic tumor-bearing mice with surgical resection after oral administration of PBS, FTPM, HF and HTPM were exhibited. Places pointed by the black solid arrow in the (**F**) were displayed appearance of white metastases in the lungs. **P* < 0.05, ***P* < 0.01, ****P* < 0.001.

and jejunum bleeding in mice (Supplementary Materials, Figure S2), but these findings were not found in other groups. This phenomenon disappeared upon the withdrawal of orally administered HF (Figure 8E).

Similar to the subcutaneous TNBC treatment by gavage, H&E staining of orthotopic tumor sections illustrated that the tumor samples treated with HF or HTPM had a larger necrotic area than those from the PBS- and FTPM-treated groups, and tumors from the HTPM-treated group still had the maximum amount of necrosis (Figure 9). Moreover, TUNEL staining of the tumor tissues clearly indicated higher apoptosis levels caused by HTPM than by other treatments. The apoptosis-related proteins such as Bcl-2, Bax, and Caspase-3 were regulated by HF and HTPM treatment but not by FTPM treatment. As shown in Figure 10, compared with HF, HTPM more significantly upregulated the expression of Bax and Caspase-3, and downregulated the expression of Bcl-2. Hence, these results demonstrated that HTPM could enhance the inhibitory effect of HF on the growth of orthotopic TNBC xenografts after surgery.

The in vivo toxicity of these treatments was also monitored by the changes in body weight and histological analysis of jejunum and lungs. Oral administration of HF, but not of HTPM or FTPM, caused a significant loss of body weight in mice, but the effect was quickly reversed three days after the withdrawal of HF. In addition, jejunum congestion was found on the H&E staining pictures from partial mice treated orally with HF but not in those treated with FTPM or HTPM, indicating that HTPM are safer and can be better used in clinical medicine. It has recently been reported that patient-derived orthotopic xenograft models of TNBC display varying degrees of distant metastatic potential, detected in the lung (20/57, 35%), liver (7/57, 12%), and brain (1/57, less than 2%).[54,55] A number of studies have also shown that orthotopic xenografts in mice generated by injecting TNBC cell line MDA-MB-231 could result in lung metastasis.[56,57] In the current study, the lungs of the tumor-bearing mice demonstrated metastatic foci, as indicated by the solid arrows on H&E slides when treated with PBS or FTPM, whereas the lungs from HF- or HTPM-treated mice exhibited normal histological features without any tumors. The metastasis in the lungs was displayed whiteness via visual inspection (Figure 8F). Compared with other groups (PBS, FTPM, and HF), the HTPM group had the lowest degree of lung metastasis, illustrating that HTPM possessed the excellent ability to inhibit the lung metastasis of TNBC. Simultaneously, compared with the lungs invaded by breast cancer parenchymal cells (black point arrow) in the PBS and FTPM groups, the lungs in the HF and HTPM groups were relatively normal (Figure 9). These results confirm that HF and HTPM can effectively impede the lung metastasis of TNBC in the orthotopic mice, which has also been reported by several previous studies.[24] For example, HF has been reported to suppress the migration and invasion of MCF-7 cells in vitro.[22] Increased TGF-β expression is a hallmark of cancer progression and it

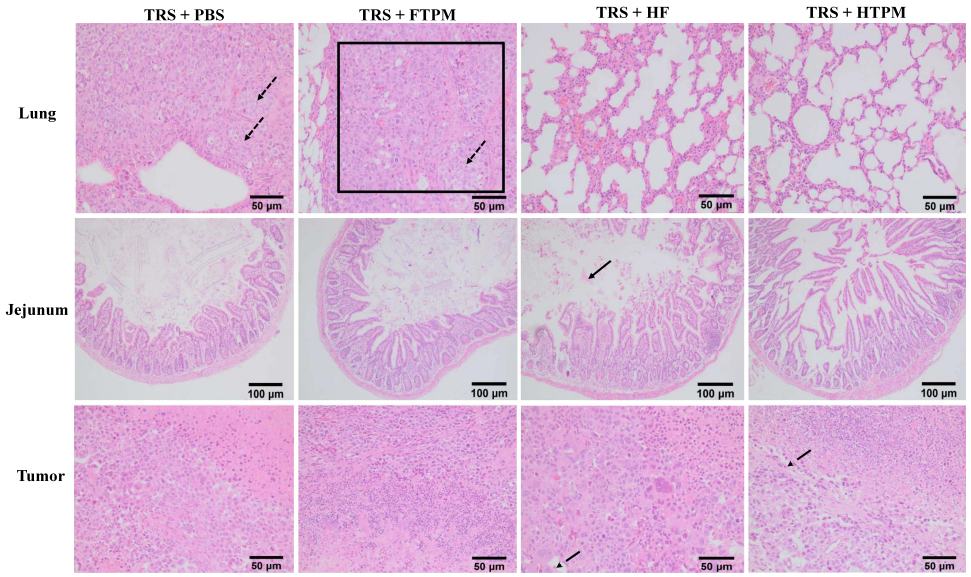

Figure 9 Histological analysis of lungs (200×), jejunums (100×) and tumors (200×) from orthotopic tumor-bearing mice treated with TRS+PBS, TRS+FTPM, TRS+HF and TRS+HTPM using H&E staining. Places pointed by the black point arrow and black box area in the lung slices picture for the TRS+PBS group and TRS+FTPM group were showed lungs appear or were filled with breast cancer parenchyma cells. Further, the place pointed by the black solid arrow in the jejunum picture of TRS+HF group represents the phenomenon of jejunum hemorrhage. Alternatively, places pointed by the black dotted arrow in the tumor picture of TRS+HF group and TRS+HTPM group demonstrate generation of apoptosis for tumor tissues. Images were taken at 200× and 100× magnification.

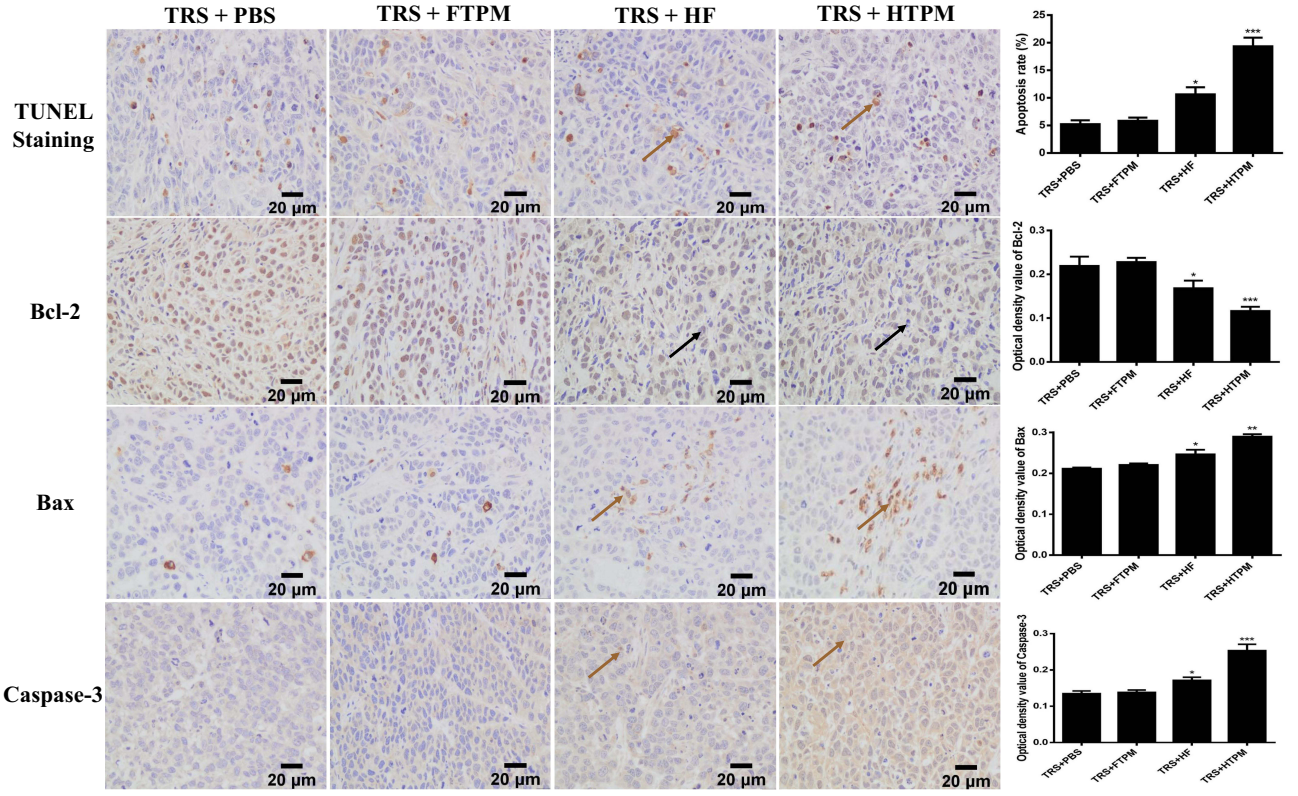

Figure 10 Apoptosis of tumor tissues from orthotopic tumor-bearing treated mice with TRS+PBS, TRS+FTPM, TRS+HF and TRS+HTPM. Places pointed by the brown solid arrow in the TUNEL Staining, bax and caspase-3 for TRS+HF and TRS+HTPM represent generation of apoptosis for tumor tissues, which appear brown color. Furthermore, Places pointed by the black solid arrow in the bcl-2 for TRS+HF and TRS+HTPM indicate anti-apoptosis for tumor tissues. Images were taken at 400× magnification. *P < 0.05, **P < 0.01, ***P < 0.001.

contributes to the invasion and metastasis of tumors, including TNBC. It is well known that HF is an inhibitor of the TGF-β/Smad3 cascade.[58] Therefore, HF has also been demonstrated to be an effective therapy for the treatment of TNBC metastasis though the inhibition of TGF-β and BMP signaling. Furthermore, HF also suppresses the transcription of the MMP-2 gene, which is associated with a marked decrease in ECM invasion in vitro and lung colonization by bladder carcinoma cells.[59] In summary, HTPM suppress the lung metastasis of TNBC and decrease the gastrointestinal toxicity of orally administered HF in orthotopic mouse models.

Conclusion

In the current study, the as-prepared HTPM with smaller sizes and a uniform distribution had the excellent stability and sustained release behavior in the simulated GI fluids. TPGS polymeric micelles not only effectively enhanced the intestinal absorption via inhibiting the efflux of P-gp but also increased the cellular permeability to HF. Indeed, compared with HF, orally administered HTPM significantly impeded GI toxicity in the subcutaneous tumor mouse models. Moreover, HTPM administered by gavage markedly strengthened the therapeutic effect of HF against the residual tissues of TNBC orthotopic xenografts after surgical resection, and more importantly, it drastically inhibited the lung metastasis of TNBC. Taken together, HTPM deserve further study to explore its therapeutic potential for treating the metastasis of TNBC patients in clinical settings.

Abbreviations

HF, halofuginone hydrobromide; HTPM, HF-loaded TPGS polymeric micelles; TNBC, triple-negative breast cancer; ER, estrogen receptor; PR, progesterone receptor; HER-2, human epidermal growth factor receptor 2; MTD, maximum tolerated dose; FDA, Food and Drug Administration; DLT, dose-limiting toxicities; EMT, epithelial-mesenchymal transition; TGF-β, transforming growth factor beta; ECM, extracellular matrix; TPGS, D-α-tocopherol polyethylene glycol 1000 succinate; FBS, fetal bovine serum; DMEM, Dulbecco's modified Eagle's medium; HD, hydrodynamic diameter; ZP, zeta potential; PDI, polydispersity index; DLS, dynamic light scattering; GI, gastrointestinal; TEER, transepithelial electrical resistance; HPLC, high performance liquid chromatography; P-gp, P-glycoprotein; P_{app}, permeability coefficient; ER, efflux ratio; NJAU, Nanjing Agricultural University; TIR, tumor inhibition rate; TRS, tumor resection surgery; FTPM, TPGS polymeric micelles without HF; DAB, diaminobenzidine; TEM, transmission electron microscopy; CRP, cumulative release percentage; ER, efflux rate; CPZ, chlorpromazine.

Acknowledgments

This work was supported by grants from the National Natural Science Foundation of China (32172918&31672612), the Fundamental Research Funds for the Central Universities (KYGD202002), the National Key Research and Development Program (2016YFD0501306), and a project funded by the Priority Academic Program Development of Jiangsu Higher Education Institutions (PAPD). We thank Let-Pub (www.letpub.com) for its linguistic assistance during the preparation of this manuscript.

Disclosure

The authors report no conflicts of interest in relation to this work and declare that they have no known competing financial interests or personal relationships that could have appeared to influence the work reported in this paper.

References

1. Yin L, Duan JJ, Bian XW, et al. Triple-negative breast cancer molecular subtyping and treatment progress. *Breast Cancer Res*. 2020;22(1):61. doi:10.1186/s13058-020-01296-5
2. Kumar P, Aggarwal R. An overview of triple-negative breast cancer. *Arch Gynecol Obstet*. 2016;293(2):247–269. doi:10.1007/s00404-015-3859-y
3. Kim C, Gao R, Sei E, et al. Chemoresistance evolution in triple-negative breast cancer delineated by single-cell sequencing. *Cell*. 2018;173(4):879–893.e13. doi:10.1016/j.cell.2018.03.041
4. Garrido-Castro AC, Lin NU, Polyak K. Insights into molecular classifications of triple-negative breast cancer: improving patient selection for treatment. *Cancer Discov*. 2019;9(2):176–198. doi:10.1158/2159-8290.CD-18-1177
5. Demiroglu-Zergeroglu A, Turhal G, Topal H, et al. Anti-carcinogenic effects of halofuginone on lung-derived cancer cells. *Cell Biol Int*. 2020;44(9):1934–1944. doi:10.1002/cbin.11399

6. Cortes J, Rugo HS, Guo Z, Karantza V, Schmid P. Pembrolizumab plus chemotherapy in triple-negative breast cancer - authors' reply. *Lancet*. 2021;398(10294):24–25. doi:10.1016/S0140-6736(21)00374-3
7. Pines M, Spector I. Halofuginone - the multifaceted molecule. *Molecules*. 2015;20(1):573–594. doi:10.3390/molecules20010573
8. Elahi-Gedwillo KY, Carlson M, Zettervall J, et al. Antifibrotic therapy disrupts stromal barriers and modulates the immune landscape in pancreatic ductal adenocarcinoma. *Cancer Res*. 2019;79(2):372–386. doi:10.1158/0008-5472.CAN-18-1334
9. Kim Y, Sundrud MS, Zhou C, et al. Aminoacyl-tRNA synthetase inhibition activates a pathway that branches from the canonical amino acid response in mammalian cells. *Proc Natl Acad Sci USA*. 2020;117(16):8900–8911. doi:10.1073/pnas.1913788117
10. Yee KO, Connolly CM, Pines M, et al. Halofuginone inhibits tumor growth in the polyoma middle T antigen mouse via a thrombospondin-1 independent mechanism. *Cancer Biol Ther*. 2006;5(2):218–224. doi:10.4161/cbt.5.2.2419
11. Xia X, Wang X, Zhang S, et al. miR-31 shuttled by halofuginone-induced exosomes suppresses MFC-7 cell proliferation by modulating the HDAC2/cell cycle signaling axis. *J Cell Physiol*. 2019;234(10):18970–18984. doi:10.1002/jcp.28537
12. de Jonge MJ, Dumez H, Verweij J, et al. Phase I and pharmacokinetic study of halofuginone, an oral quinazolinone derivative in patients with advanced solid tumours. *Eur J Cancer*. 2006;42(12):1768–1774. doi:10.1016/j.ejca.2005.12.027
13. Khalid S, Ahmad N, Khizar S, et al. Magnetic polymer colloids for ultrasensitive molecular imaging. In: *Magnetic Polymer Colloids for Ultrasensitive Molecular Imaging. Magnetic Nanoparticles in Human Health and Medicine: Current Medical Applications and Alternative Therapy of Cancer*. Wiley; 2021:978–1119754671.
14. Alomari M, Almahasheer A, Jermy BR, et al. Impact of poly (styrene-acrylic acid) latex nanoparticles on colorectal and cervical cancer cells. *Polymers*. 2021;13(13):2025. doi:10.3390/polym13132025
15. Li W, Xue J, Xu H. Combined administration of PTX and S-HM-3 in TPGS/Solutol micelle system for oncotarget therapy. *Int J Nanomedicine*. 2019;14:1011–1026. doi:10.2147/IJN.S189864
16. Lammari N, Tarhini M, Miladi K, et al. Encapsulation methods of active molecules for drug delivery. In: Chappel E, editor. *Drug Delivery Devices and Therapeutic Systems*. Academic Press; 2021:289–306.
17. Zuo R, Zhang J, Song X, et al. Encapsulating halofuginone hydrobromide in TPGS polymeric micelles enhances efficacy against triple-negative breast cancer cells. *Int J Nanomedicine*. 2021;16:1587–1600. doi:10.2147/IJN.S289096
18. Fedi A, Vitale C, Ponschin G, et al. In vitro models replicating the human intestinal epithelium for absorption and metabolism studies: a systematic review. *J Control Release*. 2021;335:247–268. doi:10.1016/j.jconrel.2021.05.028
19. Stecklair KP, Hamburger DR, Egorin MJ, et al. Pharmacokinetics and tissue distribution of halofuginone (NSC 713205) in CD2F1 mice and Fischer 344 rats. *Cancer Chemother Pharmacol*. 2001;48(5):375–382. doi:10.1007/s002800100367
20. Elkin M, Miao HQ, Nagler A, et al. Halofuginone: a potent inhibitor of critical steps in angiogenesis progression. *FASEB J*. 2000;14 (15):2477–2485. doi:10.1096/fj.00-0292com
21. Guo L, Xie G, Wang R, et al. Local treatment for triple-negative breast cancer patients undergoing chemotherapy: breast-conserving surgery or total mastectomy? *BMC Cancer*. 2021;21(1):717. doi:10.1186/s12885-021-08429-9
22. Rosenberg SM, Partridge AH. Management of breast cancer in very young women. *Breast*. 2015;24(Suppl 2):S154–158. doi:10.1016/j.breast.2015.07.036
23. Golshan M, Loibl S, Wong SM, et al. Breast conservation after neoadjuvant chemotherapy for triple-negative breast cancer: surgical results from the brightness randomized clinical trial. *JAMA Surg*. 2020;155(3):e195410. doi:10.1001/jamasurg.2019.5410
24. Xia X, Wang L, Zhang X, et al. Halofuginone-induced autophagy suppresses the migration and invasion of MCF-7 cells via regulation of STMN1 and p53. *J Cell Biochem*. 2018;119(5):4009–4020. doi:10.1002/jcb.26559
25. González-González A, Muñoz-Muela E, Marchal JA, et al. Activating transcription factor 4 modulates TGFβ-induced aggressiveness in triple-negative breast cancer via Smad 2/3/4 and mTORC2 signaling. *Clin Cancer Res*. 2018;24(22):5697–5709. doi:10.1158/1078-0432.CCR-17-3125
26. Huang H, Brekken RA. The next wave of stroma-targeting therapy in pancreatic cancer. *Cancer Res*. 2019;79(2):328–330. doi:10.1158/0008-5472.CAN-18-3751
27. Fan Z, Jiang B, Shi D, et al. Selective antitumor activity of drug-free TPGS nano-micelles with ROS-induced mitochondrial cell death. *Int J Pharm*. 2021;594:120184. doi:10.1016/j.ijpharm.2020.120184
28. Roger E, Lagarce F, Garcion E, et al. Lipid nanocarriers improve paclitaxel transport throughout human intestinal epithelial cells by using vesicle-mediated transcytosis. *J Control Release*. 2009;140(2):174–181. doi:10.1016/j.jconrel.2009.08.010
29. Chai GH, Xu Y, Chen SQ, et al. Transport mechanisms of solid lipid nanoparticles across Caco-2 cell monolayers and their related cytotoxicology. *ACS Appl Mater Interfaces*. 2016;8(9):5929–5940. doi:10.1021/acsami.6b00821
30. Wang Y. *Transport Mechanism of Polymannuronic Acid and Polyguronic Acid Across Caco-2 Cell Monolayer [D]*. Shandong University; 2020.
31. Zhang S, Pang G, Chen C, et al. Effective cancer immunotherapy by Ganoderma lucidum polysaccharide-gold nanocomposites through dendritic cell activation and memory T cell response. *Carbohydr Polym*. 2019;205:192–202. doi:10.1016/j.carbpol.2018.10.028
32. Boix-Montesinos P, Soriano-Teruel PM, Armiñán A, et al. The past, present, and future of breast cancer models for nanomedicine development. *Adv Drug Deliv Rev*. 2021;173:306–330. doi:10.1016/j.addr.2021.03.018
33. Chen Q, Wang C, Zhang X, et al. In situ sprayed bioresponsive immunotherapeutic gel for post-surgical cancer treatment. *Nat Nanotechnol*. 2019;14(1):89–97. doi:10.1038/s41565-018-0319-4
34. Yang M, Li J, Gu P, et al. The application of nanoparticles in cancer immunotherapy: targeting tumor microenvironment. *Bioact Mater*. 2020;6 (7):1973–1987. doi:10.1016/j.bioactmat.2020.12.010
35. Lu Z, Zou J, Li S, et al. Epigenetic therapy inhibits metastases by disrupting premetastatic niches. *Nature*. 2020;579(7798):284–290. doi:10.1038/s41586-020-2054-x
36. Wang H, Shi W, Zeng D, et al. pH-activated, mitochondria-targeted, and redox-responsive delivery of paclitaxel nano-micelles to overcome drug resistance and suppress metastasis in lung cancer. *J Nanobiotechnology*. 2021;19(1):152. doi:10.1186/s12951-021-00895-4
37. Xu Z, Zheng S, Gao X, et al. Mechanochemical preparation of chrysomycin a self-micelle solid dispersion with improved solubility and enhanced oral bioavailability. *J Nanobiotechnology*. 2021;19(1):164. doi:10.1186/s12951-021-00911-7
38. Fang Z, Pan S, Gao P, et al. Stimuli-responsive charge-reversal nano drug delivery system: the promising targeted carriers for tumor therapy. *Int J Pharm*. 2020;575:118841. doi:10.1016/j.ijpharm.2019.118841

39. Alomari M, Balasamy RJ, Almohazey D, et al. Nile red-poly (Methyl Methacrylate)/silica nanocomposite particles increase the sensitivity of cervical cancer cells to tamoxifen. *Polymers*. 2020;12(7):1516. doi:10.3390/polym12071516
40. Yang X, Zhang W, Jiang W, et al. Nanoconjugates to enhance PDT-mediated cancer immunotherapy by targeting the indoleamine-2,3-dioxygenase pathway. *J Nanobiotechnology*. 2021;19(1):182. doi:10.1186/s12951-021-00919-z
41. Muthu MS, Kutty RV, Luo Z, et al. Theranostic vitamin E TPGS micelles of transferrin conjugation for targeted co-delivery of docetaxel and ultra-bright gold nanoclusters. *Biomaterials*. 2015;39:234–248. doi:10.1016/j.biomaterials.2014.11.008
42. Xiong XY, Pan X, Tao L, et al. Enhanced effect of folated pluronic F87-PLA/TPGS mixed micelles on targeted delivery of paclitaxel. *Int J Biol Macromol*. 2017;103:1011–1018. doi:10.1016/j.ijbiomac.2017.05.136
43. Panyam J, Zhou WZ, Prabha S, et al. Rapid endo-lysosomal escape of poly(DL-lactide- co glycolide) nanoparticles: implications for drug and gene delivery. *FASEB J*. 2002;16(10):1217–1226. doi:10.1096/fj.02-0088com
44. National archives & records service of office. FDA draft guidance for industry on drug interaction studies-study design, data analysis, implications for dosing, and labeling recommendations. *Availability Federal Register*. 2012;77(34):9946.
45. Li XX, Wang Y, Sun NY, et al. Biopharmaceutical classification system research for six commonly used anti-parasitic drugs in chickens. *J Nanjing Agric Univ*. 2020;43(5):919–926.
46. Xie Z, Zhang Z, Lv H. Rapamycin loaded TPGS-Lecithins-Zein nanoparticles based on core-shell structure for oral drug administration. *Int J Pharm*. 2019;568:118529. doi:10.1016/j.ijpharm.2019.118529
47. Du Z, Mao Y, Zhang P, et al. TPGS-galactose-modified polydopamine co-delivery nanoparticles of nitric oxide donor and doxorubicin for targeted chemo-photothermal therapy against drug-resistant hepatocellular carcinoma. *ACS Appl Mater Interfaces*. 2021;13(30):35518–35532. doi:10.1021/acsami.1c09610
48. Neves AR, Queiroz JF, Costa Lima SA, et al. Cellular uptake and transcytosis of lipid-based nanoparticles across the intestinal barrier: relevance for oral drug delivery. *J Colloid Interface Sci*. 2016;463:258–265. doi:10.1016/j.jcis.2015.10.057
49. Bogman K, Zysset Y, Degen L, et al. P-glycoprotein and surfactants: effect on intestinal talinolol absorption. *Clin Pharmacol Ther*. 2005;77(1):24–32. doi:10.1016/j.clpt.2004.09.001
50. Beloqui A, Solinís MÁ, Gascón AR, et al. Mechanism of transport of saquinavir-loaded nanostructured lipid carriers across the intestinal barrier. *J Control Release*. 2013;166(2):115–123. doi:10.1016/j.jconrel.2012.12.021
51. Sun S, Du X, Fu M, et al. Galactosamine-modified PEG-PLA/TPGS micelles for the oral delivery of curcumin. *Int J Pharm*. 2021;595:120227. doi:10.1016/j.ijpharm.2021.120227
52. Chen T, Tu L, Wang G, et al. Multi-functional chitosan polymeric micelles as oral paclitaxel delivery systems for enhanced bioavailability and anti-tumor efficacy. *Int J Pharm*. 2020;578:119105. doi:10.1016/j.ijpharm.2020.119105
53. Zhang E, Chu F, Xu L, et al. Use of fluorescein isothiocyanate isomer I to study the mechanism of intestinal absorption of fucoidan sulfate in vivo and in vitro. *Biopharm Drug Dispos*. 2018;39(6):298–307. doi:10.1002/bdd.2137
54. Ramani VC, Lemaire CA, Triboulet M, et al. Investigating circulating tumor cells and distant metastases in patient-derived orthotopic xenograft models of triple-negative breast cancer. *Breast Cancer Res*. 2019;21(1):98. doi:10.1186/s13058-019-1182-4
55. Ameri K, Luong R, Zhang H, et al. Circulating tumour cells demonstrate an altered response to hypoxia and an aggressive phenotype. *Br J Cancer*. 2010;102(3):561–569. doi:10.1038/sj.bjc.6605491
56. Guo B, Wu S, Zhu X, et al. Micropeptide CIP2A-BP encoded by LINC00665 inhibits triple-negative breast cancer progression. *EMBO J*. 2020;39(1):e102190. doi:10.15252/embj.2019102190
57. Taras D, Blanc JF, Rullier A, et al. Halofuginone suppresses the lung metastasis of chemically induced hepatocellular carcinoma in rats through MMP inhibition. *Neoplasia*. 2006;8(4):312–318. doi:10.1593/neo.05796
58. Spector I, Zilberstein Y, Lavy A, et al. Involvement of host stroma cells and tissue fibrosis in pancreatic tumor development in transgenic mice. *PLoS One*. 2012;7(7):e41833. doi:10.1371/journal.pone.0041833
59. Zcharia E, Atzmon R, Nagler A, et al. Inhibition of matrix metalloproteinase-2 by halofuginone is mediated by the Egr1 transcription factor. *Anticancer Drugs*. 2012;23(10):1022–1031. doi:10.1097/CAD.0b013e328357d186